Int. J. Nonlinear Anal. Appl. In Press, 1–14
ISSN: 2008-6822 (electronic)
http://dx.doi.org/10.22075/ijnaa.2025.36806.5395

The efficiency assessment of output-only modal identification methods for noise-infected data

Leila Khanmohammadi*, Seyed Amin Mostafavian

Department of Civil Engineering, Faculty of Engineering, Payame Noor University, Tehran, Iran

(Communicated by Javad Vahidi)

Abstract

The modal parameters obtained from the first few vibration modes of structures have many applications. To identify these modal parameters in civil engineering structures, the output data of the structures is usually used. These data contain the structural response and some noise. The modal parameters are affected by noise in the output data. The present work has been done to assess the possibility and accuracy of identifying the modal parameters of beams in the presence of noise. To do this, the modal parameters of the different modes of single-span beams were obtained using output data with different signal-to-noise ratios. The acceleration signals were obtained by transient analysis, and then different powers of noise were generated and added to the signals. The modal parameters of the beams were obtained using Peak Picking, Frequency Domain Decomposition and Data-Driven Stochastic Subspace Identification output-only methods. Using signal-to-noise ratios of 13.98 db or greater, modal parameters were identified for all the considered modes. At a signal-to-noise ratio of -6.02 to 13.98 db (higher noise level), it was not possible to identify the modal parameters of the first mode of beams, but the parameters of the higher modes were identified with good accuracy.

Keywords: Structural identification, Output-only method, Single-span beam, Signal-to-noise ratio
2020 MSC: 60H50

1 Introduction

Structural identification has been applied to structural health monitoring, finite element model updating and damage detection [9, 46]. This procedure identifies modal parameters such as the natural frequency, mode shape and damping ratio of a structure. Output-only methods are primarily used for structural identification of structures under actual operating conditions because they have been found to have more advantages than other methods [13, 27, 28, 56]. The methods of Peak Picking (PP) [11, 25, 26], Frequency Domain Decomposition (FDD) [4, 6, 8, 17], and Data-Driven Stochastic Subspace Identification (DD-SSI) [12, 19, 24, 48, 55] are used widely for output-only estimation of modal parameters.

In order to properly obtain the modal parameters of a structure using output-only methods, the output data must be of good quality [15]. In practice, the measured outputs are the result of inputs, along with a series of unwanted data that is called "noise" [36]. To identify the modal parameters of a structure using output-only methods, output data should have an appropriate signal-to-noise ratio (SNR). As the signals induced by ambient excitation, which are

*Corresponding author
Email addresses: l.khanmohammadi@pnu.ac.ir (Leila Khanmohammadi), amin.mostafavian@gmail.com (Seyed Amin Mostafavian)

Received: February 2025 *Accepted:* April 2025

used for output-only modal identification tests, have very low levels of dynamic response (that is, signals with low power), the noise power should generally be reduced. For this purpose, appropriate data acquisition strategies must be adopted to minimize the level of noise [14, 44, 49, 50]. After good data acquisition, techniques such as filtering and averaging can be used to reduce the effect of noise [34, 39, 43].

Bonness and Jenkins [10] presented a noise removal technique with which an unlimited amount of unwanted correlated noise can be removed from a set of data by geqslantmodifying the statistical correlation relations and spectral functions.

Adeli and Jiang [31] removed noise from traffic flow data using wavelet packet transform techniques. Jiang et al. [32] developed a Bayesian discrete wavelet packet transform denoising approach based on the integration of Bayesian hypothesis testing and wavelet packet analysis. Al-Ghahtani et al. [2] extended an output-only identification of parameters of a multidimensional system from a record of noisy output measurements by using a multiwavelet denoising technique.

Despite these efforts, uncertainty in the sources and the amount of noise in practice mean it is not possible to eliminate noise completely [34, 45], therefore, identification of the modal parameters of a structure is done using noisy data. Dorvash and Pakzad [23] evaluated the effect of measurement noise on physical contribution ratio (PCR). They observed that the PCR is sensitive to the level of noise in the measured response.

Shi et al. [47] proposed a novel output-only method to estimate the structural parameters of a shear-beam building under unknown ground excitation. A three-story shear-beam building was used numerically to demonstrate the proposed technique. Two noise levels of 1% and 5% root mean square (RMS) of the noise-free signal were considered. Their result indicated that the estimation errors for stiffness coefficients are 1.41%, for 1% RMS noise and 2.42%, for 5% RMS noise, respectively.

De Roeck et al. [22] compared two system identification techniques, namely PP and SSI, for a 15-storey reinforced concrete shear core building. Their results showed that the SSI technique can detect frequencies that are possibly missed with the PP method and gives a more reasonable modal shape in most cases. Peeters et al. [40] determined the modal parameters of the Z-24 bridge via different output-only modal identification methods; two of them were PP and SSI. They found that the quality of the extracted mode shapes was higher for the SSI method than for the PP method.

Kim and Lynch [33] evaluated two output-only system identification methods, namely FDD and SSI, for a support-excited frame structure. They concluded that similar accuracy of mode shape estimation was confirmed between the time-domain SSI and frequency-domain FDD, and in the case of output-only system identification with a limited number of data points, time-domain SSI was recommended rather than frequency-domain FDD due to the low resolution issues of FDD when estimating natural frequency.

Gomaa et al. [30] compared three different techniques of output-only identification methods for extracting modal parameters of a two-story resisting steel frame; two of these methods were FDD and SSI. They found that a good agreement in identified natural frequency and mode shape existed with SSI and FDD. Andersen et al. [6] compared the performance of various output-only modal estimation methods for the identification of the Z-24 highway bridge; two of these methods were PP and SSI. The two methods seemed to agree very well on the natural frequency and mode shape estimations of the first five modes, except for the first mode, for PP couldn't identify it.

Yi and Yun [52] investigated several modal identification methods for a two-bay and 4-storey building structure. They also considered 0% to 60% noise in the root mean squares (RMS) of noise-free signals. Their numerical investigation showed that the frequency domain method (FDD) was generally more vulnerable to the measurement noise than the time domain method (TDM), and the estimates by the frequency domain method were less accurate than those by the time domain method, particularly when the two adjacent modes were closely spaced. Moreover, they included that the SSI method gave the most accurate estimates under the large measurement noise. Chen et al. [20] obtained the modal parameters of the Newmarket Viaduct bridge via different output-only methods; two of them were PP and SSI. The comparison revealed that the two methods considered gave reasonably consistent estimates of the natural frequencies and mode shapes.

These parameters, which are obtained with noisy data, are then used for structural health monitoring, finite element model updating and damage detection. In most cases, the first few modes of a structure are used [53]. In the current research, it is hypothesized that the possibility and accuracy of identifying the modal parameters of the first few modes of a structure are affected by the SNR. The effects of various SNRs on output-only identification of modal parameters were studied. For this purpose, four beams with the same geometrical and mechanical properties, but different support conditions, were considered. Band-limited white noise excitation was applied to each beam, and

the acceleration signals from the beam were obtained using transient analysis.

Using these signals, the modal parameters of the first five modes of the beams were identified using Peak Picking, Frequency Domain Decomposition and Data-Driven Stochastic Subspace Identification methods. Because less attention is paid to damping in structural health monitoring compared to the other two modal parameters (mode shape and natural frequency) [18], it was not identified.

To generate noisy data, noise having powers that differed from the signal power was added to the signals. Because of the random nature of noise, this process was repeated 100 times. The noisy data and described methods were then used to obtain the modal parameters of the beams for various SNRs.

2 Noisy data generation

Output-only structural identification is based only on the measured response of structures. This response contains the structure response and the output noise. The simplest mathematical model for considering noise in data is the additive noise model shown in Fig. 1 [42]. In this model, the output noise is modelled as zero-mean Gaussian white noise [38]. The structure response S(t), referred to herein as the signal, is corrupted by random output noise N(t). The measured response is NS(t). The output noise consists of any undesirable signal and may physically arise from measurement devices and sensors, etc. [54].

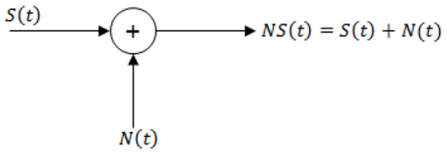

Figure 1: The additive noise model [42].

The amount of noise in the measured response affects the accuracy of the estimated modal parameters [1, 37]. The amount of noise in a signal is quantified by the SNR and is expressed in Eq. (2.1) as:

$$SNR = \frac{P_s}{P_n} \tag{2.1}$$

where P_s and P_n are the signal power and noise power, respectively, and P is the mean square of data shown in Eq.(2.2) as:

$$P = \frac{\sum_{i=1}^{n} x_i^2}{n} \tag{2.2}$$

where x_i denotes the i^{th} data sample in which n is the total number of samples. SNR may be expressed in decibels as:

$$SNR_{dB} = 10 \times log_{10}(SNR). \tag{2.3}$$

Eq. (2.4) is used to generate noise N(t)[35,41] as:

$$N(t) = RMS(S(t)) \times NL \times W(t) \tag{2.4}$$

where$RMS(S(t))$ is the root mean square (RMS) of the signals, NL is a constant that determines the noise level and $W(t)$ is a random function with the same dimensions as $S(t)$. The presence of $W(t)$ in Eq. (2.4) is due to the random nature of noise. This function has a normal distribution with a zero mean and unit standard deviation [38]. $N(t)$ is defined as such to allow parameterization of its power concerning signal power, as will be explained below. Eq. (2.4) can be rewritten in Eq. (2.5) as:

$$\begin{Bmatrix} n_1 \\ \vdots \\ n_n \end{Bmatrix} = RMS(\begin{Bmatrix} s_1 \\ \vdots \\ s_n \end{Bmatrix}) \times NL \times \begin{Bmatrix} w_1 \\ \vdots \\ w_n \end{Bmatrix} \tag{2.5}$$

where n_i, s_i and w_i are the noise, signal and random function of the i^{th} data sample, respectively. Eq. (2.5) leads to the formation of Eq. (2.6) as:

$$\begin{cases} n_1 = RMS(S(t)) \times NL \times w_1 \\ \vdots \\ n_n = RMS(S(t)) \times NL \times w_n \end{cases} \tag{2.6}$$

Squaring both sides of Eq. (2.6) and then taking the average produces:

$$\frac{\sum_{i=1}^{n} n_i^2}{n} = [RMS(S(t))]^2 \times (NL)^2 \times \frac{\sum_{i=1}^{n} w_i^2}{n}. \tag{2.7}$$

Given $RMS(S(t)) = \sqrt{P_s}$, $P_n = (\sum_{i=1}^{n} n_i^2)/n$, Eq. (2.7) can be rewritten as follows:

$$P_n = P_s \times (NL)^2 \times \frac{\sum_{i=1}^{n} w_i^2}{n}. \tag{2.8}$$

Because $W(t)$ has zero mean and unit standard deviation, $\frac{\sum_{i=1}^{n} w_i^2}{n}$ in Eq. (2.8) is equal to the variance of random function $W(t)$, which is equal to one. Eq. (2.8) then can be rewritten as follows:

$$P_n = P_s \times (NL)^2. \tag{2.9}$$

In Eq. (2.9), the noise power equals the product of the signal power and the square of the noise level. The SNR in this case is equal to the inverse of the square of the noise level as shown in Eq. (2.10):

$$SNR = \frac{P_s}{P_n} = \frac{1}{(NL)^2}. \tag{2.10}$$

In term of decibels, Eq. (2.10) may be expressed in Eq. (2.11) as:

$$SNR_{dB} = 10 \times log_{10} \frac{1}{(NL)^2} = -20 \times log_{10} NL. \tag{2.11}$$

After generating the noise and adding it to the signal, a noisy signal can be generated in Eq. (2.12) [51] as:

$$NS(t) = S(t) + N(t). \tag{2.12}$$

3 Modeling and generating noise-free data

To investigate the effect of SNR on the structural identification of single-span beams, four beams having different support conditions were considered. In Fig. 2, these beams are shown as a clamped-free supported beam (CF), simple-simple supported beam (SS), clamped-simple supported beam (CS) and clamped-clamped supported beam (CC). ANSYS finite element analysis software was used for the analysis of the beams. Of the library elements of this software, the element BEAM 188 was used for modelling the beams. BEAM 188 is a linear (2-node) beam element with six degrees of freedom at each node. The degrees of freedom at each node include translations in and rotations about the x, y, and z directions [7].

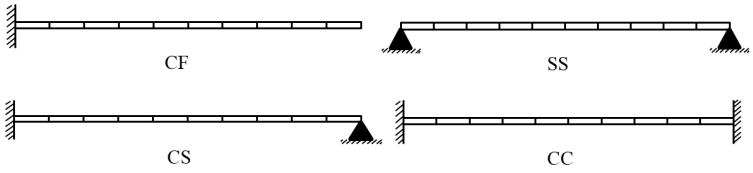

Figure 2: Finite element model of beams CF, SS, CS and CC.

Each beam was modelled in two-dimensional space with ten elements, each with a length of 100 mm and a square cross-section of 10 × 10 mm. Sensitivity analysis was used to determine that an element length of 100 mm provides acceptable accuracy for studying the modes of interest in this work. The material model behaviour of the beams is linear isotropic. The elastic modulus of the beams is $2{\times}10^{11} N/m^2$, the mass density is $7850 N.s^2/m^4$, and the Poisson's ratio is 0.3. These are typical properties of steel sections produced in Iran. The geometric properties of the beams were chosen such that the frequencies of the modes considered are sufficiently far apart.

For a validation of the finite element model in ANSYS, the analytical natural frequencies of the beam CF were obtained via the dynamic equation of a clamped-free beam subjected to free vibration [21]. The results for the first five natural frequencies of the beam CF with the relative error percentage between the modal analysis of the finite

Table 1: The first five natural frequencies of the beam CF obtained from the modal analysis and analytical method.

	Natural Frequency [Hz]		
Mode Number	Modal Analysis	Analytical method	Relative Error [%]
1^{st} Mode	8.2	8.2	0.0
2^{nd} Mode	52.2	51.2	1.9
3^{rd} Mode	152.4	144.8	4.9
4^{th} Mode	319.0	280.8	12.0
5^{th} Mode	577.3	463.7	19.7

Table 2: The first five natural frequencies of the beams SS, CS and CC obtained from the modal analysis.

Beam	Mode 1	Mode 2	Mode 3	Mode 4	Mode 5
SS	23.2	95.9	228.7	442.5	773.8
CS	36.4	123.0	274.0	513.9	885.3
CC	53.3	154.1	325.0	594.1	1011.2

element model and the analytical equation are presented in Table 1. As can be seen, the difference in the natural frequencies in higher modes is greater due to the limitation of the meshing of the finite element model.

The modal parameters for each beam were obtained using finite element modal analysis and are considered to be reference modal parameters. The first five natural frequencies of the beams SS, CS and CC are shown in Table 2.

To generate noise-free data from transient analysis of beams, each node was excited in the vertical direction using a time history force which was generated as Gaussian-banded white noise (1 to 1500 Hz) with RMS amplitudes of 0.2 Newton. The sampling time step was 0.0001 sec, and the acceleration responses were measured at a rate of 10000 Hz, resulting in a Nyquist frequency of 5000 Hz, which is higher than the largest natural frequency of all the beams in Tables 1 & 2 (1011.2 Hz). The recording duration (T) was the required time for a certain mode and can be defined as $(\omega_k \xi_k)^{-1}$ where ω_k and ξ_k are the natural frequency and damping ratio of mode k, respectively [16]. Proportional damping was assigned to the model by matching a damping ratio of 2.5% to all frequencies. As the minimum natural frequency of the beams was 8.2 Hz in Tables 1 & 2, the recording duration based on the above formula was 4.9 sec. A recording duration of 5 seconds was considered in this work.

4 Structural identification of beams with noisy data

In Section 3, the acceleration signals were obtained from the transient analysis of each beam. These signals ($S(t)$) were free of noise (zero noise level). Measurement noise $N(t)$ was modelled as zero-mean Gaussian white noise and was added to all channels of acceleration response data. The noise level was defined as the ratio of the RMS of the noise to the RMS of the noise-free acceleration response at each channel. This ratio was kept constant at all channels for a given noise level. Seven levels of measurement noise were considered here. Noise $N(t)$ was generated at different noise levels (NL) as shown in Eq. (2.4). By adding $N(t)$ to $S(t)$, as in Eq. (2.12), noisy data ($NS(t)$) was generated. The noise levels and the corresponding SNR values are shown in Table 3.

Table 3: Different noise levels and SNRdB values.

Noise Level (NL)	Signal to Noise Ratio (dB)
5%	26.02
10%	20.00
20%	13.98
50%	6.02
75%	2.50
100%	0.00
200%	-6.02

Noise generation is statistically independent; thus, because of the random characteristics of the noise, the process should be repeated [22]. A set of 100 system identification runs was performed for each beam. At each noise level,

100 noise $N(t)$ and, consequently, 100 noisy data sets $NS(t)$ were generated. The first five mode shapes of each beam were determined with the noisy data $NS(t)$ using the PP method. The modal assurance criterion (MAC) values were calculated between each of these mode shapes along with the corresponding reference mode shapes (MAC value ranges from zero to one, where one represents full compliance of the two modes [3]).

The minimum, mean and standard deviation of MAC for 100 runs of beam CF are shown in Table 4. Because the minimum values of MAC for all mode shapes of the beam at $SNRdB = 26.02$ are equal to 1, these mode shapes, as identified by PP, were in good agreement with the reference mode shapes. Table 4 shows that, for the first mode shape, decreasing SNRdB decreased the minimum and mean values of MAC and increased the standard deviations. No significant change occurred in the minimum, mean and standard deviation of MAC in other mode shapes after decreasing SNRdB. This process was performed for the SS, CS and CC beams. The noisy data with the minimum MAC value for each beam using the PP method was used to determine the modal parameters for the other methods.

The frequency resolution for PP and FDD was $1/T = 1/5Hz = 0.2Hz$. The peaks were selected manually in PP and FDD. For implementation of the SSI data-driven method, the acceleration response data was used to form an output Hankel matrix having 10 block rows with 9 or 10 rows in each block (equal to the number of acceleration channels considered). The number of block rows multiplied by the number of measurement channels will produce the maximum model order. For noisy data, several model orders were considered to build a block Hankel matrix, which was at most 200.

Table 4: Different noise levels and SNRdB values.

Mode No.	Statistical Result	SNR (dB)						
		26.02	20.00	13.98	6.02	2.50	0.00	-6.02
1^{st} Mode	Minimum	1.00	0.99	0.98	0.88	0.77	0.59	0.00
	Average	1.00	1.00	0.99	0.96	0.90	0.82	0.50
	Standard Deviation	0.00	0.01	0.03	0.15	0.31	0.64	2.17
2^{nd} Mode	Minimum	1.00	1.00	1.00	1.00	0.99	0.99	0.95
	Average	1.00	1.00	1.00	1.00	1.00	1.00	0.98
	Standard Deviation	0.00	0.00	0.00	0.00	0.01	0.02	0.03
3^{rd} Mode	Minimum	1.00	1.00	1.00	1.00	1.00	1.00	0.99
	Average	1.00	1.00	1.00	1.00	1.00	1.00	1.00
	Standard Deviation	0.00	0.00	0.00	0.00	0.00	0.00	0.01
4^{th} Mode	Minimum	1.00	1.00	1.00	1.00	1.00	1.00	1.00
	Average	1.00	1.00	1.00	1.00	1.00	1.00	1.00
	Standard Deviation	0.00	0.00	0.00	0.00	0.00	0.00	0.00
5^{rd} Mode	Minimum	1.00	1.00	1.00	1.00	1.00	1.00	0.99
	Average	1.00	1.00	1.00	1.00	1.00	1.00	1.00
	Standard Deviation	0.00	0.00	0.00	0.00	0.00	0.00	0.01

4.1 Identification of natural frequencies

The first five natural frequencies of each beam were determined using the PP, FDD and SSI methods and the results are presented in Tables 5 to 8. The second column of these tables shows the SNRdB values for the various noise levels. The differences between these values and the corresponding values shown in Table 3 are due to the random characteristics of $W(t)$ in Eq. (2.3). The MATLAB function randn was used to generate the random function W(t). Because the random numbers generated have no exact zero means and unit standard deviations, the resulting SNRdB values may differ slightly from values in Table 3. For example, for beam CF, the SNRdB for a noise level of 5% was 26.08 instead of 26.02, which is a difference of 0.23%.

The natural frequencies of noise-free beams are presented in row NL = 0 in Tables 5 to 8. In this case, the SNRdB value is denoted by an infinity symbol. In Tables 5 to 8, some natural frequencies were not identified (as denoted by a dash). It can be seen that FDD performed better for noisy data than the other methods because it obtained more natural frequencies. For example, the first natural frequency of beam CF was obtained at a noise level of 50%, while such a frequency was identified using PP and SSI at 20% and 5%, respectively.

Table 5: The identified natural frequencies of beam CF (Hz)

Noise Level (NL)	SNR_{dB}	Frequency of Mode 1			Frequency of Mode 2			Frequency of Mode 3			Frequency of Mode 4			Frequency of Mode 5		
		PP	FDD	SSI	PP	FDD	SSI	PP	FDD	SSI	PP	FDD	SSI	PP	FDD	SSI
0	∞	8.0	7.3	8.1	52.0	51.3	52.1	152.0	151.4	152.2	318.0	317.4	317.8	571.0	571.3	571.1
5%	26.08	8.0	7.3	8.3	52.0	51.3	52.2	152.0	151.4	152.2	318.0	317.4	317.1	571.0	571.3	571.1
10%	20.10	8.0	7.3	-	52.0	51.3	52.0	152.0	151.4	152.2	318.0	317.4	317.8	571.0	571.3	570.9
20%	13.95	8.0	7.3	-	52.0	51.3	52.4	152.0	151.4	152.2	318.0	317.4	317.8	571.0	571.3	571.1
50%	6.05	-	7.3	-	52.0	51.3	55.8	152.0	151.4	152.3	318.0	317.4	317.8	571.0	571.3	571.1
75%	2.46	-	-	-	52.0	51.3	54.1	152.0	151.4	152.5	318.0	317.4	317.8	571.0	571.3	571.0
100%	0.04	-	-	-	52.0	51.3	55.4	152.0	151.4	152.5	318.0	317.4	318.2	571.0	571.3	571.3
200%	-6.02	-	-	-	52.0	51.3	55.7	152.0	151.4	150.9	318.0	317.4	317.4	571.0	571.3	571.5

Table 6: The identified natural frequencies of beam SS (Hz)

Noise Level (NL)	SNR_{dB}	Frequency of Mode 1			Frequency of Mode 2			Frequency of Mode 3			Frequency of Mode 4			Frequency of Mode 5		
		PP	FDD	SSI	PP	FDD	SSI	PP	FDD	SSI	PP	FDD	SSI	PP	FDD	SSI
0	∞	23.0	22.0	23.6	96.0	95.2	96.0	228.5	229.5	228.2	439.5	439.5	439.2	759.0	759.3	758.9
5%	25.96	23.0	22.0	23.6	96.0	95.2	96.0	228.5	229.5	228.2	439.5	439.5	439.2	759.0	759.3	758.9
10%	20.13	23.0	22.0	23.9	96.0	95.2	96.0	228.5	229.5	228.5	439.5	439.5	439.5	759.0	759.3	758.8
20%	13.88	23.0	22.0	23.3	96.0	95.2	96.1	228.5	229.5	228.5	439.5	439.5	439.4	759.0	759.3	757.8
50%	5.93	23.0	22.0	-	96.0	95.2	96.6	228.5	229.5	228.8	439.5	439.5	439.4	759.0	759.3	759.1
75%	2.48	23.0	22.0	-	96.0	95.2	96.6	228.5	229.5	228.8	439.5	439.5	439.5	759.0	759.3	759. 4
100%	0.09	-	-	-	96.0	95.2	96.0	228.5	229.5	228.8	439.5	439.5	439.4	759.0	759.3	759.3
200%	-6.02	-	-	-	96.0	95.2	96.1	228.5	229.5	229.0	439.5	439.5	439.5	759.0	759.3	759.0

Table 7: The identified natural frequencies of beam CS (Hz)

Noise Level (NL)	SNR_{dB}	Frequency of Mode 1			Frequency of Mode 2			Frequency of Mode 3			Frequency of Mode 4			Frequency of Mode 5		
		PP	FDD	SSI	PP	FDD	SSI	PP	FDD	SSI	PP	FDD	SSI	PP	FDD	SSI
0	∞	36.5	36.6	36.4	123.0	122.1	122.9	273.5	273.4	273.3	509.5	510.3	509.7	863.5	864.3	863.8
5%	26.09	36.5	36.6	36.4	123.0	122.1	122.9	273.5	273.4	273.3	509.5	510.3	509.7	863.5	864.3	863.8
10%	20.09	36.5	36.6	36.3	123.0	122.1	122.9	273.5	273.4	273.3	509.5	510.3	509.7	863.5	864.3	863.5
20%	13.98	36.5	36.6	36.7	123.0	122.1	122.9	273.5	273.4	273.3	509.5	510.3	509.7	863.5	864.3	863.6
50%	6.14	36.5	36.6	-	123.0	122.1	123.0	273.5	273.4	273.3	509.5	510.3	510.4	863.5	864.3	863.7
75%	2.50	36.5	36.6	-	123.0	122.1	122.8	273.5	273.4	273.3	509.5	510.3	510.3	863.5	864.3	863.6
100%	-0.09	-	-	-	123.0	122.1	122.7	273.5	273.4	273.3	509.5	510.3	510.4	863.5	864.3	864.0
200%	-6.02	-	-	-	123.0	122.1	123.8	273.5	273.4	274.0	509.5	510.3	510.2	863.5	864.3	864.0

Table 8: The identified natural frequencies of beam CC (Hz)

Noise Level (NL)	SNR_{dB}	Frequency of Mode 1			Frequency of Mode 2			Frequency of Mode 3			Frequency of Mode 4			Frequency of Mode 5		
		PP	FDD	SSI	PP	FDD	SSI	PP	FDD	SSI	PP	FDD	SSI	PP	FDD	SSI
0	∞	53.5	53.7	53.3	154.0	153.8	154.0	324.0	324.7	323.9	587.5	588.4	587.3	979.0	979.0	979.1
5%	26.04	53.5	53.7	53.3	154.0	153.8	154.0	324.0	324.7	323.9	587.5	588.4	587.3	979.0	979.0	979.1
10%	20.01	53.5	53.7	53.1	154.0	153.8	154.0	324.0	324.7	323.9	587.5	588.4	587.4	979.0	979.0	979.1
20%	13.92	53.5	53.7	53.7	154.0	153.8	154.1	324.0	324.7	323.9	587.5	588.4	587.4	979.0	979.0	978.1
50%	5.98	53.5	53.7	53.8	154.0	153.8	154.1	324.0	324.7	324.0	587.5	588.4	587.5	979.0	979.0	978.8
75%	2.46	53.5	53.7	52.9	154.0	153.8	154.1	324.0	324.7	324.0	587.5	588.4	587.4	979.0	979.0	979.0
100%	0.09	-	53.7	-	154.0	153.8	153.8	324.0	324.7	323.9	587.5	588.4	587.1	979.0	979.0	978.7
200%	-6.02	-	-	-	154.0	153.8	153.8	324.0	324.7	323.8	587.5	588.4	589.4	979.0	979.0	979.0

It can be seen from Tables 5 to 8 that the natural frequency of the first mode of the beams was identified using PP, FDD and SSI methods for the SNR values of ≥13.98, ≥-6.02, and ≥26.02, respectively.

As shown in Tables 5 to 8, increasing the noise level did not alter the natural frequencies identified using FDD and PP. Gkoktsi et al. [29] obtained the modal parameters of a simply-supported beam using FDD for SNRs of 10 and 20 db. They found that the noise level did not significantly affect the natural frequency estimation in these SNRs. In the frequency domain methods (PP and FDD), the natural frequency of the structure was obtained from the peak value of the ANPSD diagram. The ANPSD diagram for beam CF is shown in Fig. 3 for NL = 0% to 200%. The last free node (node 11) of the beam was used as the reference channel. Fig. 3 shows that, although the different noise levels produced different ANPSD diagrams, the peak location or values of the natural frequencies of the beams did not change.

The absolute value of the percentage of relative error between the identified natural frequencies (Tables 5 to 8) and the reference natural frequencies of the beams (Table 1 & 2) was determined and is presented in Table 9. For the SSI method, the mean percentage of relative error for various noise levels is presented. Other than the error of the natural frequency of the first mode of beams CF and SS identified by FDD, the errors are very small.

Table 9: The relative error between the identified and reference natural frequency for the beams (%).

Beam	Method	Frequency of Mode 1	Frequency of Mode 2	Frequency of Mode 3	Frequency of Mode 4	Frequency of Mode 5
CF	PP	2.4	0.4	0.3	0.3	1.1
	FDD	10.9	1.7	0.7	0.5	1.0
	SSI	1.2	3.0	0.2	0.4	1.1
SS	PP	0.9	0.1	0.1	0.7	1.9
	FDD	5.2	0.7	0.3	0.7	1.9
	SSI	1.3	0.3	0.1	0.7	1.9
CS	PP	0.3	0.0	0.2	0.8	2.4
	FDD	0.5	0.7	0.2	0.7	2.4
	SSI	0.3	0.2	0.2	0.8	2.4
CC	PP	0.4	0.1	0.3	1.1	3.2
	FDD	0.8	0.5	0.1	1.0	3.2
	SSI	0.5	0.1	0.3	1.1	3.2

4.2 Identification of mode shapes

As stated, the first five mode shapes of each beam were identified using the noisy data having a minimum MAC value using the PP method. The MAC values between these mode shapes and the corresponding reference mode shapes are presented in Table 10. A value of 1 in the NL = 0% row indicates good agreement between the identified mode shapes and the corresponding reference mode shapes for the noise-free case. As shown in Table 10, as the noise level increased, the MAC values either decreased or remained constant. The lower values for MAC for the first mode shape of each beam show that this mode of the beams was not identified appropriately at high noise levels. Because the MAC values close to or equal to the one obtained by FDD are greater than those for the other two methods, this method is more appropriate for the identification of the mode shapes of the beams in the case of noisy data.

Figs. 4 to 8 show the acceptable minimum value for MAC for the first five mode shapes of beam CF identified by PP for the various noise levels, together with the corresponding reference mode shapes. As PP identified the mode shapes for each node, these figures can be interpolated between two nodes. Fig. 4 shows that mode shapes up to a noise level of 20%(SNR ≥ 13.98) are an appropriate approximation of the first mode shape of beam CF. Figs. 5 to 8 show that the other mode shapes of this beam are in good agreement with the corresponding reference mode shapes up to a noise level of 200% (SNR ≥ -6.02). Table 10 and the figures show that 0.95 is the defined MAC threshold. It was found that this value is constant for the other methods and the other beams.

As for the mode shapes, the first natural frequency and other frequencies of the beam CF were also obtained by PP at noise levels of 20% and 200%, respectively (Table 5). The mode shape was properly identified for the previously identified corresponding natural frequency. For example, the first mode shape of beam CF was identified by PP at a noise level of 20% and the corresponding natural frequency was also identified at this noise level. This was also done for the other beams and methods. The natural frequencies identified in Tables 5 to 8 have corresponding MAC values of ≥0.95 (Table 10). For example, in Tables 5 to 8, the second to fourth natural frequencies of each beam for all noise levels were identified. Their MAC values in Table 10 are all ≥0.95.

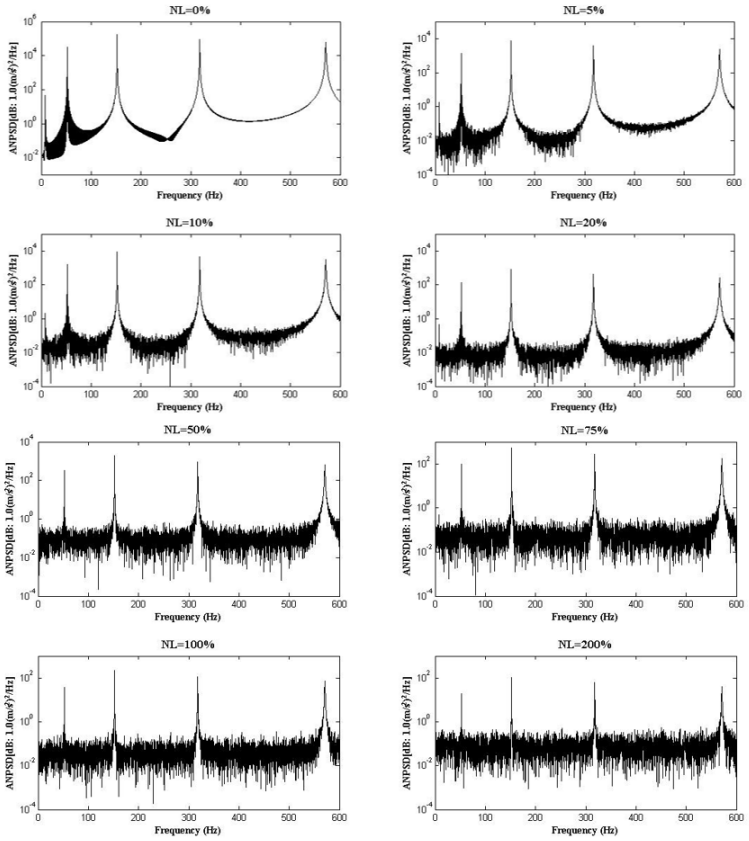

Figure 3: The ANPSD diagram for beam CF for various noise levels

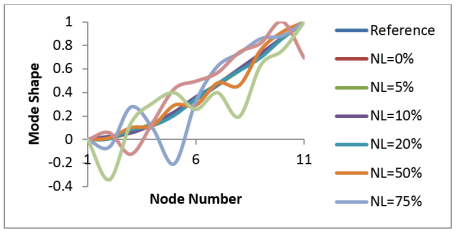

Figure 4: The first mode shape of beam CF

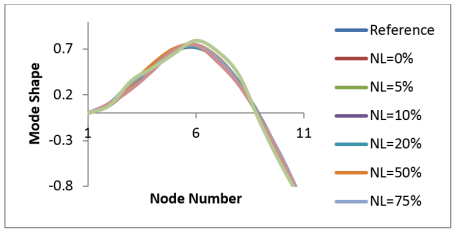

Figure 5: The second mode shape of beam CF

5 Conclusion

To investigate the effect of noise on modal parameter identification, noise with different powers was added to the acceleration signals of beams and the noisy data was generated. This process was repeated 100 times. The modal parameters of the beams were identified for all 100 noisy data sets. The natural frequencies of all modes of each beam except the first mode were identified for all noise levels. The natural frequency of the first mode was determined using the PP, FDD and SSI methods for SNR values of $\geq$13.98, $\geq$-6.02 and $\geq$26.02, respectively. The natural frequencies

Table 10: The MAC values between the identified mode shapes and the corresponding reference mode shapes.

Mode No.	NL	SNR_{dB}	Beam CF			Beam SS			Beam CS			Beam CC		
			PP	FDD	SSI	PP	FDD	SSI	PP	FDD	SSI	PP	FDD	SSI
1^{st} Mode	0%	∞	1.00	1.00	1.00	1.00	1.00	1.00	1.00	1.00	1.00	1.00	1.00	1.00
	5%	26.02	1.00	1.00	0.98	1.00	1.00	1.00	1.00	1.00	1.00	1.00	1.00	1.00
	10%	20.00	0.99	1.00	0.86	1.00	1.00	0.99	1.00	1.00	0.99	1.00	1.00	1.00
	20%	13.98	0.98	1.00	0.84	1.00	1.00	0.97	1.00	1.00	0.96	1.00	1.00	0.99
	50%	6.02	0.88	0.99	0.65	0.99	0.99	0.88	0.99	1.00	0.92	1.00	1.00	0.99
	75%	2.50	0.77	0.94	0.58	0.98	0.99	0.63	0.99	1.00	0.88	0.99	1.00	0.98
	100%	0.00	0.59	0.84	0.34	0.34	0.97	0.38	0.92	0.99	0.42	0.92	0.99	0.84
	200%	-6.02	0.00	0.27	0.12	0.01	0.95	0.00	0.00	0.94	0.29	0.50	0.88	0.36
2^{nd} Mode	0%	∞	1.00	1.00	1.00	1.00	1.00	1.00	1.00	1.00	1.00	1.00	1.00	1.00
	5%	26.02	1.00	1.00	1.00	1.00	1.00	1.00	1.00	1.00	1.00	1.00	1.00	1.00
	10%	20.00	1.00	1.00	1.00	1.00	1.00	1.00	1.00	1.00	1.00	1.00	1.00	1.00
	20%	13.98	1.00	1.00	0.99	1.00	1.00	1.00	1.00	1.00	1.00	1.00	1.00	1.00
	50%	6.02	1.00	1.00	0.99	1.00	1.00	1.00	1.00	1.00	1.00	1.00	1.00	1.00
	75%	2.50	0.99	1.00	0.98	1.00	1.00	1.00	1.00	1.00	1.00	1.00	1.00	1.00
	100%	0.00	0.99	1.00	0.97	1.00	1.00	0.99	1.00	1.00	0.99	1.00	1.00	1.00
	200%	-6.02	0.95	1.00	0.95	0.99	1.00	0.98	1.00	1.00	0.99	1.00	1.00	0.99
3^{rd} Mode	0%	∞	1.00	1.00	1.00	1.00	1.00	1.00	1.00	1.00	1.00	1.00	1.00	1.00
	5%	26.02	1.00	1.00	1.00	1.00	1.00	1.00	1.00	1.00	1.00	1.00	1.00	1.00
	10%	20.00	1.00	1.00	1.00	1.00	1.00	1.00	1.00	1.00	1.00	1.00	1.00	1.00
	20%	13.98	1.00	1.00	1.00	1.00	1.00	1.00	1.00	1.00	1.00	1.00	1.00	1.00
	50%	6.02	1.00	1.00	1.00	1.00	1.00	1.00	1.00	1.00	1.00	1.00	1.00	1.00
	75%	2.50	1.00	1.00	1.00	1.00	1.00	1.00	1.00	1.00	1.00	1.00	1.00	1.00
	100%	0.00	1.00	1.00	0.99	1.00	1.00	1.00	1.00	1.00	1.00	1.00	1.00	1.00
	200%	-6.02	0.99	1.00	0.99	0.98	1.00	0.98	1.00	1.00	1.00	1.00	1.00	1.00
4^{th} Mode	0%	∞	1.00	1.00	1.00	1.00	1.00	1.00	1.00	1.00	1.00	1.00	1.00	1.00
	5%	26.02	1.00	1.00	1.00	1.00	1.00	1.00	1.00	1.00	1.00	1.00	1.00	1.00
	10%	20.00	1.00	1.00	1.00	1.00	1.00	1.00	1.00	1.00	1.00	1.00	1.00	1.00
	20%	13.98	1.00	1.00	1.00	1.00	1.00	1.00	1.00	1.00	1.00	1.00	1.00	1.00
	50%	6.02	1.00	1.00	1.00	1.00	1.00	1.00	1.00	1.00	1.00	1.00	1.00	1.00
	75%	2.50	1.00	1.00	1.00	1.00	1.00	1.00	1.00	1.00	1.00	0.99	1.00	0.98
	100%	0.00	1.00	1.00	1.00	1.00	1.00	1.00	1.00	1.00	1.00	0.99	1.00	0.98
	200%	-6.02	1.00	1.00	0.99	0.99	1.00	1.00	0.99	1.00	0.99	0.97	0.99	0.96
5^{th} Mode	0%	∞	1.00	1.00	1.00	1.00	1.00	1.00	1.00	1.00	1.00	1.00	1.00	1.00
	5%	26.02	1.00	1.00	1.00	1.00	1.00	1.00	1.00	1.00	1.00	1.00	1.00	1.00
	10%	20.00	1.00	1.00	1.00	1.00	1.00	1.00	1.00	1.00	1.00	1.00	1.00	1.00
	20%	13.98	1.00	1.00	1.00	1.00	1.00	1.00	0.99	1.00	1.00	1.00	1.00	1.00
	50%	6.02	1.00	1.00	1.00	1.00	1.00	1.00	0.96	1.00	0.99	1.00	1.00	1.00
	75%	2.50	1.00	1.00	1.00	1.00	1.00	1.00	0.96	0.98	0.97	1.00	1.00	0.99
	100%	0.00	1.00	1.00	0.99	1.00	1.00	0.99	0.95	0.98	0.95	0.99	1.00	0.99
	200%	-6.02	0.99	1.00	0.98	0.99	1.00	0.99	0.95	0.96	0.95	0.96	1.00	0.96

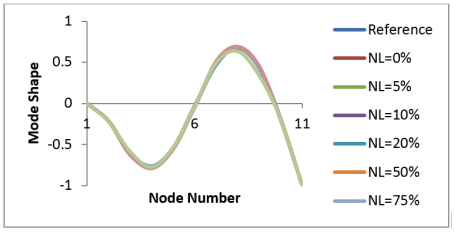

Figure 6: The third mode shape of beam CF

of the beams identified by the PP and FDD methods remained unchanged compared to the noise-free case. FDD was more powerful for identifying the natural frequencies of the beams because it identified the natural frequencies at higher noise levels compared to the other two methods. All results obtained for the identification of the natural frequencies of the beams held true for the corresponding mode shapes; that is, a mode shape was appropriately identified for every corresponding natural frequency. The MAC values between the properly identified mode shapes and the corresponding reference mode shapes were $\geq$0.95.

Modal parameters of the first few modes of a structure are used for structural health monitoring, finite element model updating and damage detection. The results of this study have shown that the accuracy of the first five modes

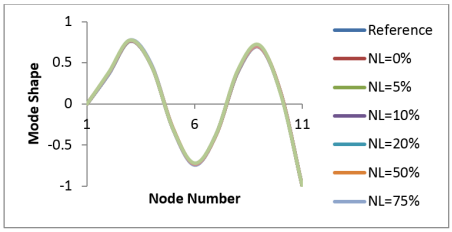

Figure 7: The fourth mode shape of beam CF

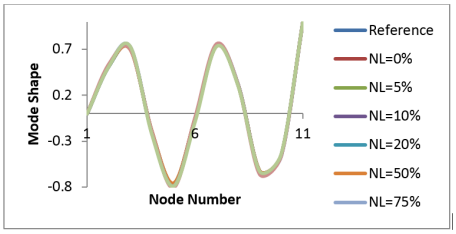

Figure 8: The fifth mode shape of beam CF

identified varies according to the amount of noise in the data. Because the amount of noise is unknown in practice, the parameters of the higher modes identified using output-only methods are more reliable than for the first mode of the beams. It is important to note that these results hold true for this particular structural system, mesh length and noise model generation. However, further studies have shown that changing the reference channel, beam section height, recording duration, sampling time, response of the beam and RMS amplitudes of input excitation does not change the results.

References

[1] H. Adeli and X. Jiang, *Dynamic Fuzzy Wavelet Neural Network Model for Structural System Identification*, J. Struct. Engin. **132** (2006), 102–111.

[2] O. Al-Gahtani, M. El-Gebeily, and Y. Khulief, *Output-only identification of system parameters from noisy measurements by multiwavelet denoising*, Adv. Mech. Engin. **6** (2014), 218328.

[3] R.J. Allemang, *The modal assurance criterion: Twenty years of use and abuse*, Sound Vib. **37** (2003), 14–21.

[4] S. Amador, M. Ørum, T. Friis, and M. Brincker, *Application of frequency domain decomposition identification technique to half spectral densities*, Topics in Modal Analysis and Testing, Conf. Proc. Soc.r Exper. Mech. Ser. (Mains M., Dilworth B., ed.), vol. 9, Springer, 2019,

[5] P. Andersen, R. Brincker, M. Goursat, and L. Mevel, *Automated modal parameter estimation for operational modal analysis of large systems*, Proc. 2nd Int. Oper. Modal Anal. Conf., vol. 1, 2007, pp. 299–308.

[6] P. Andersen, R. Brincker, B. Peeters, G. De Roeck, L. Hermans, and C. Krämer, *Comparison of system identification methods using ambient bridge test data*, Proc. 17th Int. Modal Anal. Conf., 1999, pp. 7–10.

[7] *ANSYS Documentation*, Mechanical APDL, Element Reference, Element Library, BEAM 188.

[8] M. Batel, *Operational modal analysis-another way of doing modal testing*, Sound Vib. **36** (2002), no. 8, 22–27.

[9] I. Behmanesh and B. Moaveni, *Accounting for environmental variability, modeling errors, and parameter estimation uncertainties in structural identification*, J. Sound Vib. **374** (2016), 92–110.

[10] W.K. Bonness and D.M. Jenkins, *Removing unwanted noise from operational modal analysis data*, Topics Modal Anal. **10** (2015), 115–122.

[11] R. Brincker, *Some elements of operational modal analysis*, Shock Vib. **4** (2014), 1–11.

[12] R. Brincker and P. Andersen, *Understanding stochastic subspace identification*, Proc. 24th Int. Modal Anal. Conf., 2006, pp. 279–311.

[13] R. Brincker and P.H. Kirkegaard, *Special issue on Operational Modal Analysis*, Mech. Syst. Signal Process. **24** (2010), 1209–1212.

[14] R. Brincker, T. Lago, P. Andersen, and C. Ventura, *Improving the classical geophone sensor element by digital correction*, Proc. 23th Int. Modal Anal. Conf.: Conf. Expos. Struct. Dyn., vol. 31, 2005.

[15] R. Brincker and C. Ventura, *Introduction to Operational Modal Analysis*, First ed., First edition, John Wiley and Sons, New Jersey, United States, 2015.

[16] R. Brincker, C. Ventura, and P. Andersen, *Why output-only modal testing is a desirable tool for a wide range of practical applications*, Proc. 21th Int. Modal Anal. Conf., vol. 265, 2003.

[17] R. Brincker, l. Zhang, and P. Andersen *Modal identification of output-only systems using frequency domain decomposition*, Smart Mater. Struct. **10** (2001), no. 3, 441–445.

[18] M.S. Cao, G.G. Sha, and Y.F. Gao, *Ostachowicz W., Structural damage identification using damping: a compendium of uses and features*, Smart Mater. Struct. **26** (2017), no. 4, 043001

[19] E.P. Carden and A. Mita, *Challenges in developing confidence intervals on modal parameters estimated for large civil infrastructure with stochastic subspace identification*, Struct. Control Health Monitor. **18** (2011), 53–78.

[20] X. Chen, P. Omenzetter, and S. Beskhyroun, *Comparison of output-only methods for modal identification of a twelve-span viaduct*, Proc. 5th Int. Oper. Modal Anal. Conf., 2013.

[21] A.K. Chopra, *Dynamics of Structures: Theory and Applications to Earthquake Engineering*, Third ed., Prentice Hall, USA, 2007.

[22] G. De Roeck, B. Peeters, and W.X. Ren, *Benchmark study on system identification through ambient vibration measurements*, Proc. 18th Int. Modal Anal. Conf., 2000, pp. 1106–1112.

[23] S. Dorvash and S.N. Pakzad, *Effects of measurement noise on modal parameter identification*, Smart Mater. Struct. **21** (2012), no.6, 1–15.

[24] E.P.B. Reynders, *Uncertainty quantification in data-driven stochastic subspace identification*, Mech. Syst. Signal Process. **151** (2021), 107338.

[25] J. Enriquez-Zárate, G. Valencia-Palomo, F.-R. López-Estrada, G. Silva-Navarro, J.A. Hoyo-Montaño, *Efficient predictive vibration control of a building-like structure*, Asian J. Control **22** (2020), 1411–1421.

[26] A.J. Felber, *Development of a Hybrid Bridge Evaluation System*, University of British Columbia, 1994.

[27] M. Ghobadi, M. Majji, and E. Esfahani, *AOSID: An analytical solution to the output-only system identification problem to estimate physical parameters and unknown input simultaneously*, Struct. Control Health Monitor. **24** (2017), 1–23.

[28] D.F. Giraldo, W. Song, S.J. Dyke, and J.M. Caicedo, *Modal identification through ambient vibration: Comparative study*, J. Engin. Mech. **135** (2009), 759–770.

[29] K. Gkoktsi, A. Giaralis, and B. TauSiesakul, *Sub-Nyquist signal-reconstruction-free operational modal analysis and damage detection in the presence of noise*, Proc. Sensors Smart Struct. Technol. Civil Mech. Aerospace Syst., vol. 9803, 2016.

[30] F. Gomaa, M. Tayel, K. Kandil, and G. Hekal, *Validation study illustrates the accuracy of operational modal analysis identification*, Int. J. Emerg. Technol. Adv. Engin. **11** (2012), no. 2, 658–667.

[31] X. Jiang and H. Adeli, *Wavelet packet-autocorrelation function method for traffic flow pattern analysis*, Comput.-Aid. Civil Infrast. Engin. **19** (2004), no. 5, 324–337.

[32] X. Jiang, S. Mahadeva, and H. Adeli, *Bayesian wavelet packet denoising for structural system identification*, Struct. Control Health Monitor. **14** (2007), 333–356.

[33] J. Kim and P.L. Jerome, *Comparison study of output-only subspace and frequency-domain methods for system identification of base excited civil engineering structures*, Civil Engin. Topics **4** (2011), 305–312.

[34] M. Makki Alamdari, J. Li, and B. Samali, *FRF-based damage localization method with noise suppression approach*, J. Sound Vibr. **333** (2014), 3305–3320.

[35] M. Makki Alamdari, B. Samali, J. Li, H. Kalhori, and S. Mustapha, *Spectral-based damage identification in structures under ambient vibration*, J. Comput. Civil Engin. **30** (2016), no. 4, 04015062.

[36] P. Mellinger, M. Dohler, and L. Mevel, *Variance estimation of modal parameters from output-only and input/output subspace-based system identification*, J. Sound Vibr. **379** (2016), 1–27.

[37] B. Moaveni and E. Asgarieh, *Deterministic-stochastic subspace identification method for identification of nonlinear structures as time-varying linear systems*, Mech. Syst. Signal Process. **31** (2012), 40–55.

[38] B. Moaveni, A.R. Barbos, J.P. Conte, and F.M. Hemez, *Uncertainty analysis of system identification results obtained for a seven-story building slice tested on the UCSD-NEES shake table*, Struct. Control Health Monitor. **21** (2014), 466–483.

[39] B. Peeters, B. Cornelis, K. Janssens, and H. Van Der Auweraer, *Removing disturbing harmonics in operational modal analysis*, Proc. 2nd Int. Oper. Modal Anal. Conf., 2007, pp. 1–2.

[40] B. Peeters, G. De Roeck, L. Hermans, T. Wauters, C. Krämer, and C. De Smet, *Comparison of system identification methods using operational data of a bridge test*, Proc. Int. Seminar Modal Anal., vol. 2, 1999, pp. 923–930.

[41] M.J. Perry and C.G. Koh, *Output-only structural identification in time domain: Numerical and experimental studies*, Earthquake Engin. Struct. Dyn. **37** (2008), 517–533.

[42] J.G. Proakis and M. Salehi, *Digital Communications*, Fifth ed., McGraw-Hill, New York, 2007.

[43] C. Rainieri and G. Fabbrocino, *Automated output-only dynamic identification of civil engineering structures*, Mech. Syst. Signal Process. **24** (2010), 678–695.

[44] C. Rainieri and G. Fabbrocino, *Operational modal analysis for the characterization of heritage structures*, Geofizika **28** (2018), no. 1, 109–126.

[45] E. Reynders and G. De Roeck, *Reference-based combined deterministic-stochastic subspace identification for experimental and operational modal analysis*, Mech. Syst. Signal Process. **22** (2008), 617–637.

[46] A. Sadhu, S. Narasimhan, and J. Antoni, *A review of output-only structural mode identification literature employing blind source separation methods*, Mech. Syst. Signal Process. **94** (2017), 415–431.

[47] Y. Shi, Z. Li, and C.C. Chang, *Output-only subspace identification of structural properties and unknown ground excitation for shear-beam buildings*, Adv. Mech. Engin. **8** (2016), no. 11, 1–15.

[48] H. Shokravi, H. Shokravi, N. Bakhary, M. Heidarrezaei, S.S. Rahimian Koloor, and M. Petrů, *Application of the subspace-based methods in health monitoring of civil structures: A systematic review and meta-analysis*, Appl. Sci. **10** (2020), no. 10, 3607.

[49] C. Stephan, *Sensor placement for modal identification*, Mech. Syst. Signal Process. **27** (2012), 461–470.

[50] L. Wang, R. Song, Y. Wu, and W. Hu, *Statistically filtering data for operational modal analysis under ambient vibration in structural health monitoring systems*, MATEC Web Conf., vol. 68, 2016, pp. 14010.

[51] Z. Wu and N.E. Huang, *Ensemble empirical mode decomposition: A noise-assisted data analysis method*, Adv. Adapt. Data Anal. **1** (2009), no. 1, 1–41.

[52] J.H. Yi and C.B. Yun, *Comparative study on modal identification methods using output-only information*, Struct. Engin. Mech. **17** (2004), no. 3-3, 445–66.

[53] X. Zhu and H. Hao, *Development of an integrated structural health monitoring system for bridge structures in operational conditions*, Front. Struct. Civil Engin. **6** (2012), no. 3, 321–333.

[54] J. Zhang, J. Prader, K.A. Grimmelsman, F. Moon, A.E. Aktan, and A. Shama, *Experimental vibration analysis for structural identification of a long-span suspension bridge*, J. Engin. Mech. **139** (2013), 748–759.

[55] G. Zhang, B. Tang, and G. Tang, *An improved stochastic subspace identification for operational modal analysis*, Measurement **45** (2012), 1246–1256.

[56] F.L. Zhang, H.B. Xiong, W.X. Shi, and X. Ou, *Structural health monitoring of Shanghai Tower during different stages using a Bayesian approach*, Struct. Control Health Monitor. **23** (2016), 1366–1384.